Validity of the Wigner-Seitz approximation in neutron star crust

N. Chamel
Institut d'Astronomie et d'Astrophysique, Université Libre de Bruxelles, CP226, Boulevard du Triomphe, 1050 Brussels, Belgium

S. Naimi, E. Khan, and J. Margueron
Institut de Physique Nucléaire, Université Paris-Sud, IN$_2$P$_3$-CNRS, F-91406 Orsay Cedex, France
(Dated: July 3, 2007)

Since the seminal work of Negele and Vautherin, the Wigner-Seitz approximation has been widely applied to study the inner crust of neutron stars formed of nuclear clusters immersed in a neutron sea. In this article, the validity of this approximation is discussed in the framework of the band theory of solids. For a typical cell of ^{200}Zr, present in the external layers of the inner crust, it is shown that the ground state properties of the neutron gas are rather well reproduced by the Wigner-Seitz approximation, while its dynamical properties depend on the energy scale of the process of interest or on the temperature. It is concluded that the Wigner-Seitz approximation is well suited for describing the inner crust of young neutron stars and the collapsing core of massive stars during supernovae explosions. However the band theory is required for low temperature transport properties as, for instance, the effective neutron mass giving rise to entrainment effects.

PACS numbers: 97.60.Jd,26.60.+c,21.10.Ma,21.60.Jz,71.15.Ap,71.18.+y,21.10.-k
Keywords: neutron star crust, band theory, Wigner-Seitz approximation, Hartree-Fock

In the standard model of neutron stars [1], the crust is believed to be formed of nuclear clusters in a body centered cubic lattice stabilized by Coulomb forces and considered infinite and pure (made of only one type of nuclei at a given density). In the inner crust, at densities above $\sim 4.10^{11}$ g.cm^{-3} and below $\sim 10^{14}$ g.cm^{-3}, the "neutron drip" regime is reached and the clusters are surrounded by a neutron fluid. A formal comparison can be made with electrons in ordinary solids present on earth: part of the neutrons participate to the nuclear clusters which form the lattice (equivalent to electrons bounded to atoms) while part of the neutrons are delocalized over the whole crystal (equivalent to valence electrons). As a consequence, the band theory of solids developed in condensed matter [2] can be applied to describe the crust of neutron star. But due to the highly specific numerical issues of band theory, nuclear physicists have preferred to use an approximation due to Wigner and Seitz (W-S) [3, 4], where the crust is divided into independent and spherical cells. Since the work of Negele and Vautherin [5], the W-S approximation has been used to predict the structure of the crust, the pairing properties, the thermal effects, or the low lying energy excitation spectrum [6, 7, 8, 9, 10, 11, 12]. Only recently, band theory calculations have been carried out in order to study the hydrodynamical properties of the neutron fluid and in particular the neutron effective mass giving rise to entrainment effects [13, 14, 15], although these calculations are not yet self-consistent. While the W-S approximation is well justified below the "neutron drip" regime, its validity beyond remains to be assessed.

In this article, we investigate the limitations of the W-S approximation in the $\rho \sim 7.10^{11}$ g.cm^{-3} density layer of the inner crust, composed of a crystal of zirconium like clusters [5] surrounded by the neutron gas. In Sect. I, before discussing the W-S approximation, we briefly review the band theory of solids. Then we compare in Sect. II the results of the band theory with those of the W-S approximation for the single particle wavefunctions and energy spectra. Consequences for the properties of the neutron gas are discussed.

I. MICROSCOPIC QUANTUM DESCRIPTION OF NEUTRON STAR INNER CRUST

An accurate description of the inner crust, assuming that it is a perfect crystal, should rely on the band theory of solids [2]. In this section, we briefly review this theory in the context of neutron star crust and discuss the W-S approximation in this framework.

A. Band theory of solids

According to the Floquet-Bloch theorem, the single particle quantum states are given by modulated plane waves

$$\varphi_{\alpha\boldsymbol{k}}(\boldsymbol{r}) = u_{\alpha\boldsymbol{k}}(\boldsymbol{r}) e^{\mathrm{i}\boldsymbol{k}\cdot\boldsymbol{r}}\,, \tag{1}$$

where the functions $u_{\alpha\boldsymbol{k}}(\boldsymbol{r})$ have the full periodicity of the lattice. Each single particle quantum state is thus labeled by a discrete index α and by a wave vector $\boldsymbol{k}$. The energy spectrum is therefore formed of a series of sheets or "bands" in $\boldsymbol{k}$-space.

The Bloch states (1) are completely determined by the knowledge of the functions $u_{\alpha\boldsymbol{k}}(\boldsymbol{r})$ inside a W-S cell of the lattice, whose shape is imposed by the symmetry of the crystal. The cell, centered around one nuclear cluster, is electrically neutral and therefore contains as many

electrons as protons. The effects of the ion lattice on the electrons, which give rise to complicated band structures in ordinary terrestrial matter are negligible in the inner crust of a neutron star due to the very high densities [16]. Nevertheless, the neutron band effects due to nuclear inhomogeneities cannot be ignored.

In the present study, we consider the outermost layers of the inner crust where pairing effects are negligible [17]. In the Hartree-Fock approximation with Skyrme forces which we shall consider in the following, the occupied nucleon single particle wave functions are obtained by solving the self-consistent equations ($q = n, p$ for neutrons and protons respectively)

$$h_0^{(q)} \varphi_{\alpha \boldsymbol{k}}^{(q)}(\boldsymbol{r}) = \varepsilon_{\alpha \boldsymbol{k}}^{(q)} \varphi_{\alpha \boldsymbol{k}}^{(q)}(\boldsymbol{r}) \tag{2}$$

where the single particle Hamiltonian is defined by

$$h_0^{(q)} \equiv -\boldsymbol{\nabla} \cdot \frac{\hbar^2}{2m_q^{\oplus}(\boldsymbol{r})} \boldsymbol{\nabla} + U_q(\boldsymbol{r}) - \mathrm{i} \boldsymbol{W_q}(\boldsymbol{r}) \cdot \boldsymbol{\nabla} \times \boldsymbol{\sigma} \,, \tag{3}$$

the effective masses $m_q^{\oplus}(\boldsymbol{r})$, mean fields $U_q(\boldsymbol{r})$ and spin-orbit terms $\boldsymbol{W_q}(\boldsymbol{r})$ being functionals of the single particle wave functions. These equations have to be solved inside the W-S cell with the boundary conditions imposed by the Floquet-Bloch theorem

$$\varphi_{\alpha \boldsymbol{k}}^{(q)}(\boldsymbol{r} + \boldsymbol{T}) = e^{\mathrm{i} \boldsymbol{k} \cdot \boldsymbol{T}} \varphi_{\alpha \boldsymbol{k}}^{(q)}(\boldsymbol{r}) \,, \tag{4}$$

where $\boldsymbol{T}$ is any lattice vector. This means in particular that the wavefunction between two opposite faces of the cell has a phase shift $e^{\mathrm{i} \boldsymbol{k} \cdot \boldsymbol{T}}$ where $\boldsymbol{T}$ is the corresponding lattice vector. The single particle energies are periodic in the reciprocal lattice whose vectors $\boldsymbol{K}$ satisfy $\boldsymbol{K} \cdot \boldsymbol{T} = 2\pi n$ (where n is any integer)

$$\varepsilon_{\alpha, \boldsymbol{k}+\boldsymbol{K}}^{(q)} = \varepsilon_{\alpha \boldsymbol{k}}^{(q)} \,. \tag{5}$$

Consequently only the values of $\boldsymbol{k}$ inside the first Brillouin zone (*i.e.* W-S cell of the reciprocal lattice) are relevant.

Equivalently, equations (2) can be written directly for the $u_{\alpha \boldsymbol{k}}^{(q)}(\boldsymbol{r})$ functions in the decomposition (1) which leads to

$$(h_0^{(q)} + h_{\boldsymbol{k}}^{(q)}) u_{\alpha \boldsymbol{k}}^{(q)}(\boldsymbol{r}) = \varepsilon_{\alpha \boldsymbol{k}}^{(q)} \, u_{\alpha \boldsymbol{k}}^{(q)}(\boldsymbol{r}) \tag{6}$$

where the $\boldsymbol{k}$-dependent Hamiltonian $h_{\boldsymbol{k}}^{(q)}$ is defined by

$$h_{\boldsymbol{k}}^{(q)} \equiv \frac{\hbar^2 k^2}{2m_q^{\oplus}(\boldsymbol{r})} + \boldsymbol{v_q} \cdot \hbar \boldsymbol{k} \,, \tag{7}$$

and the velocity operator $\boldsymbol{v_q}$ is defined by the commutator

$$\boldsymbol{v_q} \equiv \frac{1}{\mathrm{i}\hbar} [\boldsymbol{r}, h_0^{(q)}] \,. \tag{8}$$

The band theory takes into account all the symmetries of the system. However equations (2) with the boundary conditions (4) are numerically very complicated to solve. The approximation introduced a long time ago by Wigner and Seitz in the study of metallic sodium [3, 4] has been widely applied in the context of neutron star crust, as described below.

B. Wigner-Seitz approximation

The spherical W-S approximation is a computationally very efficient method with the advantage of reducing the 3D partial differential Eqs. (2) to ordinary differential radial equations. This approximation is twofold. First of all, the Hamiltonian $h_{\boldsymbol{k}}^{(q)}$ in equation (6) is neglected. Consequently the wave functions and the energies are independent of $\boldsymbol{k}$ and approximated by the solutions at $\boldsymbol{k} = 0$. Only the band index α remains. Secondly, the W-S polyhedron is replaced by a sphere of equal volume. The equations are then usually solved with the Dirichlet-Neumann mixed boundary conditions which yield a nearly constant neutron density outside the cluster.

The W-S approximation turns out to be very good if the boundary conditions play a minor role. For instance, bound states whose associated wave functions are vanishingly small outside the clusters are very well treated provided that the spatial extent of these states is smaller than the lattice spacing. This condition is fulfilled almost everywhere in the crust except in the bottom layers where the clusters nearly touch. The aim of this paper is to investigate the validity of the W-S approximation for the outermost layers of the inner crust where the bound neutron states are not altered by the boundary conditions.

Let us emphasize that in the W-S approximation, the nuclear clusters are supposed to be spherical while in the full band theory, no assumption is made about their shape. For the low densities of interest in this study, the nuclear clusters can still be considered as spherical. It should mentioned that in a recent development of the W-S approximation [18], the W-S cell is replaced by a cube with strictly periodic boundary conditions. Possible deformations of the nuclear clusters are thus included but at the price of unphysical boundary conditions because the W-S cell of the body centered cubic lattice is a truncated octahedron and not a cube (the cube being the W-S cell of the simple cubic lattice). This is the reason why we still consider the spherical W-S approximation closer to the physical situation than the cubic one at low density.

II. COMPARISON BETWEEN THE BAND THEORY AND THE W-S APPROXIMATION

The comparison between the band theory and the W-S approximation gives an estimate of the contribution (7) of the k-dependent Hamiltonian $h_{\boldsymbol{k}}$ and incidentally on the effects of the boundary conditions. We have considered the shallow layers of the crust at the average baryon density $\rho \sim 7 \times 10^{11}$ g/cm^3 formed of a crystal made of zirconium like clusters ($Z = 40$) with 160 neutrons (bound and unbound) per lattice site[5]. In the following we shall refer to such cluster as ^{200}Zr. Under such conditions, only unbound neutrons are sensitive to the

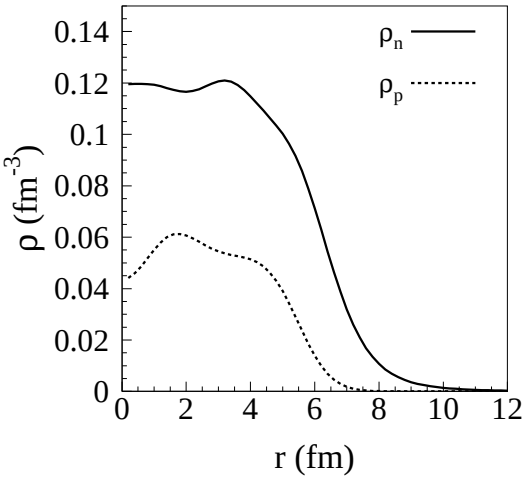

FIG. 1: Neutron (full lines) and proton (dotted lines) density distributions for ^{200}Zr in the W-S cell, obtained in the W-S approximation.

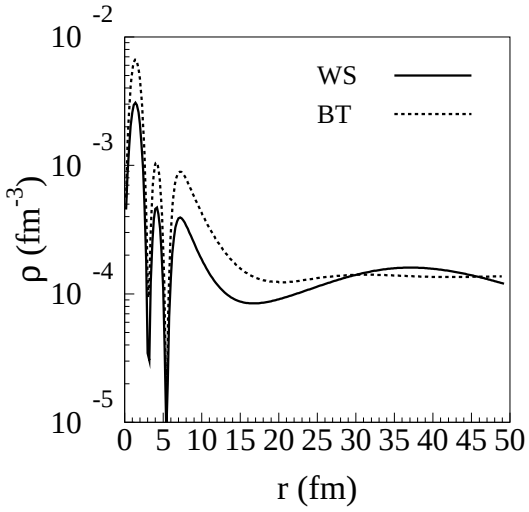

FIG. 2: Unbound neutron density calculated with the W-S approximation (WS, full lines) and the full band theory (BT, dotted lines).

boundary conditions and the nuclear clusters are spherical.

For the comparison, we first solve the self-consistent Hartree-Fock equations in coordinate space, considering the W-S approximation. The effective force used is the same as in references [7, 8, 9], namely the Skyrme interaction SLy4 [19]. In Fig. 1, we show the neutron and proton densities calculated in the spherical W-S cell with ^{200}Zr. The size of the box is $R_{\rm cell} = 49.2$ fm. The cell exhibits a very large and diffuse neutron skin, which is typical of those systems [5]. A small but non-zero neutron density is present at large radius generating a non-zero mean field potential. Asymptotically, this potential is equal to -0.05 MeV. All the states with energy larger than -0.05 MeV are therefore unbound or "free". We found that among the 160 neutrons per lattice site, 70 are unbound.

The effective mass $m_n^{\oplus}(\boldsymbol{r})$ and the mean field potential $U_n(\boldsymbol{r})$ obtained for the spherical cell are used to construct an effective Schrödinger equation for band theory calculations. As the spin-orbit splitting is weak for most of the states (see Fig. 5), we set the spin-orbit potential $\boldsymbol{W_n}(\boldsymbol{r})$ to zero. In order to study the effects of the boundary conditions, the Schrödinger equation is solved with no further iterations by imposing the Bloch boundary conditions (4) and using the Linearized Augmented Plane Wave method (see [15] for details). The coordinate space is divided in two regions: a spherical region around the cluster plus an interstitial region. In the latter region, the wave functions are expanded on a plane wave basis in order to fulfill the Bloch boundary conditions. The lattice spacing is determined by requiring that the volume of the W-S sphere is equal to the volume of the exact W-S cell of the crystal, assumed to be a body centered cubic lattice[1].

In the following, we compare the single particle wave functions and energy spectra of the unbound neutrons.

A. Single particle wavefunctions

As already discussed in Sect. I B, the wave functions of the bound states are nearly independent of the boundary conditions. As a consequence, we expect that the band theory and the W-S approximation provide identical bound states. Since the unbound states are orthogonal to the bound states, the W-S approximation and the band theory are expected to yield similar unbound wavefunctions inside the nuclear clusters. This is confirmed by the calculation of the density distribution of the unbound neutrons (whose single particle energies exceed -0.05 MeV as discussed previously) shown on Fig. 2, obtained with the band theory and the W-S approximation. For the comparison, the density $\rho(\boldsymbol{r})$ obtained from the band theory, has been averaged over the solid angle around one lattice site as follows

$$\rho(r) = \int \frac{\mathrm{d}\Omega}{4\pi} \rho(\boldsymbol{r}) \,, \tag{9}$$

where r is the radial distance from the lattice site. Similar density oscillations are obtained in both calculations

in the vicinity of the nuclear cluster for $r < 10$ fm as expected. Qualitative differences in the neutron density are however observed in the interstitial regions outside clusters due to different boundary conditions. The unbound neutron density distribution is nearly flat in the band theory while it is more fluctuating in the W-S approximation. The Bloch wavefunctions outside the clusters are similar to plane waves (thus giving a constant density) which cannot be properly described in the W-S approximation owing to the expansion of the wavefunctions into only a few spherical harmonics. An analysis of the contribution of each single particle wave function to the unbound neutron density in the W-S approximation reveals that the oscillations at small radius are mainly coming from p-states, such as $3p_{1/2}$ or $3p_{3/2}$ whereas at larger radii ($r > 20$ fm) only a few larger ℓ states, mainly d-f-g-h states, are contributing to the free neutron density.

As a result, the W-S approximation predicts a different number of neutrons outside the cluster than in the band theory. Since the total number of free neutrons should be the same in both calculations, the difference in the density profile at large radius implies a larger difference in magnitude at small radius. This is more clearly seen on Fig. 3, by plotting the integrated number $N(r)$ of free neutrons inside the W-S cell at radius r, defined by

$$N(r) = 4\pi \int_0^r r'^2 \rho(r') \mathrm{d}r' \,, \tag{10}$$

$\rho(r)$ being the local density of *unbound* neutrons. The figure shows that the W-S approximation underestimates the number $N_{\rm in} = N(R)$ of free neutrons inside the region of radius R around the cluster and consequently overestimates the number $N_{\rm out} = N(R_{\rm cell}) - N(R)$ of free neutrons outside. For both calculations, the number of free neutrons in the cell is $N(R_{\rm cell}) = 70$. Quantitatively taking $R = 15$ fm, the difference between the two calculations is about $\Delta N = |\Delta N_{\rm in}| = |\Delta N_{\rm out}| = 3$ which is rather small.

This first comparison shows that the single particle wave functions of unbound neutrons are qualitatively well reproduced by the W-S approximation inside the nuclear clusters. The main differences in the wavefunctions between the two calculations are found in the interstitial region due to the different boundary conditions. However this has a rather small effect on the ground state properties of the neutron gas, like the neutron density distribution. More generally the W-S approximation can be expected to be a good approximation to the full band theory for evaluating the matrix elements of any operator taking vanishing values outside the cluster region.

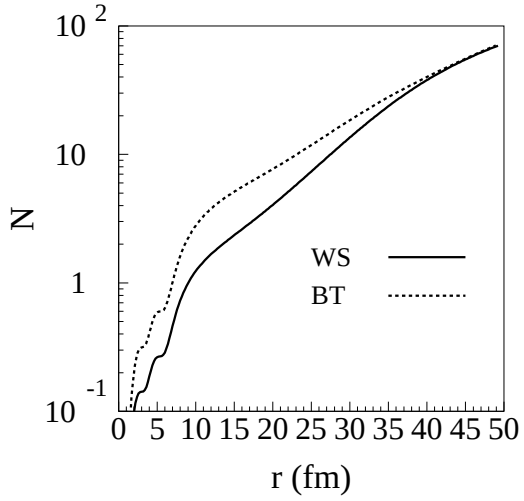

FIG. 3: Integrated unbound neutron number (see text) calculated with the W-S approximation (WS, full lines) and the band theory (BT, dotted lines)

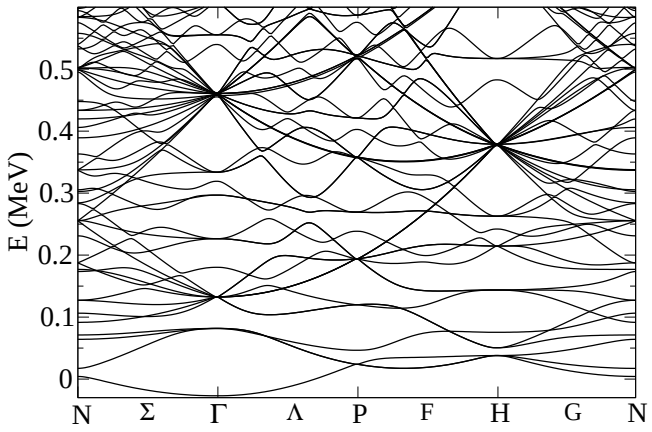

FIG. 4: Unbound single particle energy spectrum as obtained in the band theory vs the Bloch wave vector $\boldsymbol{k}$, along high symmetry lines in the first Brillouin zone using standard notations [20].

B. Single particle energy spectrum

Figs. 4 and 5 show the energy spectrum of the unbound neutrons obtained in the band theory and in the W-S approximation, respectively. It should be noted from Fig. 5 that the spin-orbit splitting is very weak for d, f, g and h states (as predicted by Negele&Vautherin [5]) but not for p states. This is due to the fact that the spin-orbit splitting is proportional to the convolution of the density gradient together with the wave functions. The density gradient is localized in the central cluster while the d, f, g and h states are mostly in the external region. For those

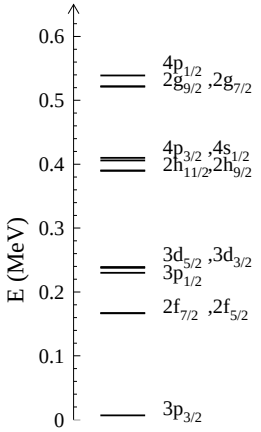

FIG. 5: Unbound single particle energy spectrum obtained in the W-S approximation.

states, the convolution leads to a weak splitting.

Since in band theory, the energies depend also on the wavevector $\boldsymbol{k}$, only the energy bands along some specific symmetry directions in $\boldsymbol{k}$-space are displayed. The energy spectrum obtained with the W-S approximation is comparable to the one obtained in the band theory for the symmetry point Γ corresponding to the center $\boldsymbol{k} = 0$ of the first Brillouin zone (W-S cell of the reciprocal lattice). The correspondence is not exact and the differences come from the spherical approximation. As a result, the W-S approximation predicts less states but with larger degeneracies than the band theory at the symmetry point Γ. The figures show clearly another important difference between the band theory and the W-S approximation: in the former case the energy spectrum is continuous while in the latter case it is discrete.

A relevant quantity to compare the energy spectra is the level density, which plays a pivotal role when calculating dynamical processes. It is defined by

$$g(E) = V_{\rm cell} \sum_{\alpha} \int_{\rm BZ} \frac{{\rm d}^3\boldsymbol{k}}{(2\pi)^3} \delta(E - \varepsilon_{\alpha\boldsymbol{k}}) \qquad (11)$$

where the integral is taken over the first Brillouin zone (BZ).

Using the δ function to integrate out one of the variables, the level density becomes

$$g(E) = \frac{V_{\rm cell}}{(2\pi)^3} \sum_{\alpha} \int \frac{{\rm d}\mathcal{S}(E)}{|\nabla_{\boldsymbol{k}} \varepsilon_{\alpha\boldsymbol{k}}|} \,, \qquad (12)$$

where the integral is taken over the surface of constant energy $\varepsilon_{\alpha\boldsymbol{k}} = E$ in $\boldsymbol{k}$-space. Expression (12) shows that the level density is a probe of the topology of constant energy surfaces in $\boldsymbol{k}$-space. We have extracted the level density from band theory by using the Gilat-Raubenheimer method as in reference [14, 15].

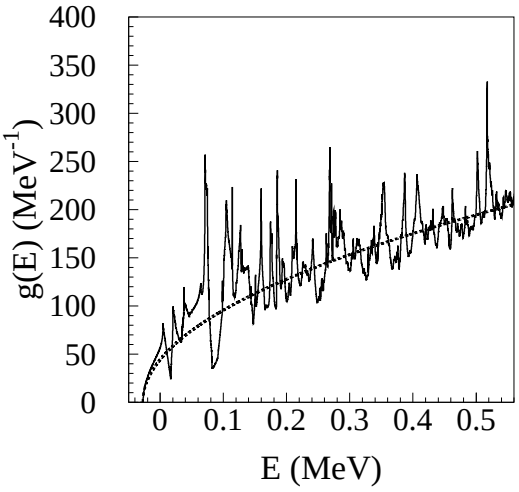

FIG. 6: Level density for neutron unbound states calculated with the band theory (solid line) compared with the prediction of the free Fermi gas (dashed line). The energy resolution is of the order of keV.

In the W-S approximation the level density reduces to a discrete sum

$$g_{\rm WS}(E) = \sum_{nj\ell} (2j+1) \delta(E - \varepsilon_{nj\ell}) \,. \qquad (13)$$

In Fig. 6, we show the level density predicted by the band theory for the unbound single particle levels. As expected the figure shows that the energy spectrum in the band theory is continuous and has a complex fine structure. The spectrum exhibits a quasi band gap of about 30 keV slightly around 90 keV. This is in sharp contrast with the W-S approximation for which the energy levels are discrete and separated by about 100 keV. In other words, the W-S approximation overestimates the neutron shell effects. The global energy dependence of the level density follows the behavior of the free Fermi gas,

$$g(E) \simeq \frac{V_{\rm cell}}{2\pi^2} \left(\frac{2m}{\hbar^2} \right)^{3/2} \sqrt{E - E_v} \,, \qquad (14)$$

where $E_v \simeq -0.031$ MeV is the energy at the bottom of the valence band. The agreement between the two curves is very good for energies close to E_v. This means that the Fermi surface is nearly spherical at low energies as confirmed by the calculations shown on Fig. 7. This is due to the fact that the Fermi wavelength of the unbound neutrons is much larger at low energies than the lattice spacing. As a consequence the effect of Bragg diffraction is negligible. It can be inferred from Fig. 6 that distortions of the Fermi surface from the spherical

FIG. 7: (Color online)Constant neutron energy surface of a body centered cubic lattice of ^{200}Zr inside the first Brillouin zone for $E = -0.0015$MeV.

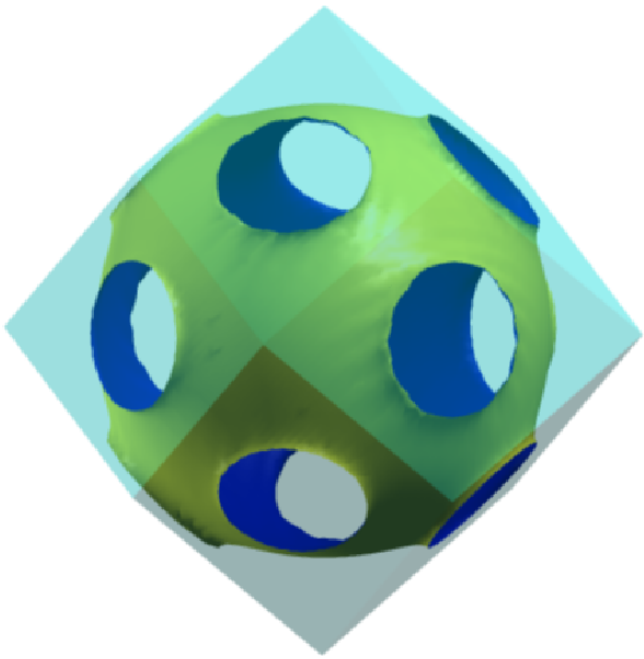

FIG. 8: (Color online)Constant neutron energy surface of a body centered cubic lattice of ^{200}Zr inside the first Brillouin zone for $E = 0.0085$MeV.

shape happens at energies larger than 0. The first kink around the zero of energy is a characteristic van Hove singularity (as a result of the vanishing of the gradient $\nabla_{\boldsymbol{k}}\, \varepsilon_{\alpha \boldsymbol{k}}$ at some $\boldsymbol{k}$ points in the expression (12), also visible on Fig. 4) and indicates a topological transition of the Fermi surface. This occurs when the Fermi sphere touches the faces of the first Brillouin zone. For a body centered cubic lattice, the transition takes place when the radius of the sphere is equal to $\sqrt{2}\pi/a$ where a is the lattice spacing. Above the first kink, the Fermi surface becomes non spherical with the appearance of necks close to the Brillouin zone faces as illustrated on Fig. 8. The Fermi surface undergoes further topological changes as it crosses Bragg planes (higher Brillouin zones) as revealed by the singularities in the level density. The actual Fermi surface (associated with the 160 neutrons per cell) has a very complicated shape with 11 branches (associated with the 11 bands which cross the Fermi level).

In Fig. 9, we show the integrated number of single particle levels which are below a given energy E

$$N(E) = \int_{E_v}^{E} d\varepsilon\, g(\varepsilon)\,. \tag{15}$$

The W-S approximation exhibits a stair steps structure due to the discretization of the states. As already noticed, the energy levels are discrete and highly degenerate, due to the imposed spherical symmetry around the cluster. In contrast, in the band theory the spherical symmetry is partly broken due to the translational symmetry of the crystal lattice. The energy levels thus broaden into bands, with a low residual degeneracy (at most 6 at each $\boldsymbol{k}$ point for cubic crystals, counting the spin degeneracy [20]), which overlap so that the energy spectrum is continuous.

In conclusion, for processes which involve transfered energies above the characteristic level spacing around the Fermi energy, the differences between the W-S approximation and the full band theory are expected to be small. For instance, it is typically the case for neutrino response function [22] or thermal effects before the star cools completely down. However at lower energies, as pertaining for instance the effective neutron mass relevant for fluid dynamics [13, 14, 15], the full band theory is required. The level spacing can be roughly evaluated from the quantity $\hbar^2/2mR^2_{\rm cell}$. From the top to the bottom layers of the crust, the characteristic level spacing varies from about 100 keV to 200 keV, which corresponds to temperatures of the order of 10^9 K. Such temperatures are found in young neutron stars less than a few hundred years after their birth [23]. The W-S approximation is therefore well suited for describing the hot dense matter (except for the high density layers where the spherical approximation may be too restrictive) in young neutron stars and in the collapsing core of massive stars during supernova explosions [6]. This discussion however does not take into account pairing effects, which are negligible in the outermost layers of the crust considered in this work but are expected to be important in denser and deeper layers [17]. It should be noted that a recent study has shown that the pairing properties of the unbound

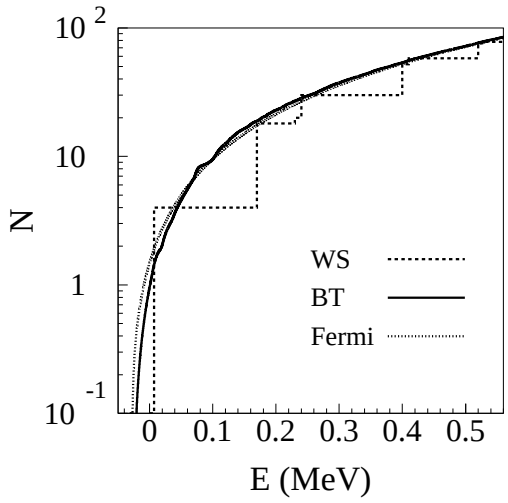

FIG. 9: Integrated state number calculated with the W-S approximation (WS, dashed lines), band theory (BT, solid line), and free Fermi gas (doted lines)

neutrons are strongly sensitive to the choice of boundary conditions in the W-S approximation, especially in the bottom layers of the crust [12, 21].

III. CONCLUSION

In this article, a comparison has been done between the full band theory and the W-S approximation which has been widely applied in studies of neutron star crust. The external layers of the inner crust at a baryon density $\rho \sim 7 \times 10^{11}$ g/cm^3 composed of zirconium like clusters ^{200}Zr have been considered. Since the bound nucleons are not much affected by the boundary conditions, we have focused on the unbound neutrons. We have shown that the ground state properties such as the unbound neutron density distribution, are rather well reproduced by the W-S approximation, while the dynamical properties depend on the process of interest or the energy exchanged. It should also be noticed that depending on the quantities of interest, the free neutron model for the unbound neutrons could be a good first approximation. In the future, it could be interesting to explore an intermediate scheme which goes beyond the Wigner-Seitz approximation and remains simpler to implement in numerical calculations than the full band theory.

The energy spectrum is continuous in the full band theory with no energy gaps while the W-S approximation yields a discrete spectrum thereby overestimating neutron shell effects. The W-S approximation can therefore be applied whenever the processes under considerations involve energies larger than the level spacing induced by the discretization, which in the present case is of order ~ 100 keV. In particular, the W-S approximation is well suited for describing the hot ($T \gtrsim 10^9$ K) dense matter in the inner crust of young neutron stars and in the collapsing core of massive stars during supernovae explosions. However low temperature transport processes such as the effective neutron mass relating the momentum to the velocity and giving rise to entrainment effects, require a fine knowledge of the energy spectrum around the Fermi level (*i.e.* the Fermi surface) which cannot be reproduced by the W-S approximation. Since the lattice spacing is predicted to decrease with increasing depth, becoming comparable to the size of the nuclear clusters and to the Fermi wave length of the free neutrons at the bottom of the crust, the validity of the W-S approximation should be carefully investigated in the denser layers of the crust, especially concerning pairing effects. Besides, the assumption of spherical symmetry in the W-S approximation is probably too restrictive near the crust-core interface where the clusters are expected to be strongly deformed [16].

Acknowledgments

N. C. gratefully acknowledges financial support from a Marie Curie Intra European fellowship (contract number MEIF-CT-2005-024660). The authors acknowledge valuable discussions with N. Sandulescu, M. Pearson and S. Goriely during the completion of this work.

[1] G.A. Baym, H.A. Bethe and C.J. Pethick, Nucl. Phys. **A 175** (1971), 225.
[2] C. Kittel, *Introduction to solid state physics*, 7th edition, Wiley&Sons (1996).
[3] E.P. Wigner and F. Seitz, Phys. Rev. **43**, 804 (1933).
[4] E.P. Wigner and F. Seitz, Phys. Rev. **46**, 509 (1934).
[5] J.W. Negele and D. Vautherin, Nucl. Phys. **A 207** (1973), 298.
[6] P. Bonche, D. Vautherin, Nucl. Phys. **A 372** (1981), 496.
[7] N. Sandulescu, N. Van Giai and R.J. Liotta, Phys. Rev. **C 69**, 045802 (2004).
[8] N. Sandulescu, Phys. Rev. **C 70**, 025801 (2004).
[9] E. Khan, N. Sandulescu and N. Van Giai, Phys. Rev. **C 71**, 042801(R) (2005).
[10] E. Vigezzi, F. Barranco, R.A. Broglia, G. Colò, G. Gori and F. Ramponi, Nucl. Phys. **A 752** (2005), 600.
[11] M. Baldo, U. Lombardo, E.E. Saperstein and S.V. Tolokonnikov, Nucl. Phys. **A 750** (2005), 409.

[12] M. Baldo, E.E. Saperstein and S.V. Tolokonnikov, Nucl.Phys. **A 775** (2006), 235.
[13] B. Carter, N. Chamel, P. Haensel, Nucl. Phys. **A 748** (2005), 675.
[14] N. Chamel, Nucl.Phys. **A 747** (2005), 109.
[15] N. Chamel, Nucl.Phys. **A 773** (2006), 263.
[16] C.J. Pethick and D.G. Ravenhall, Ann. Rev. Nucl. Part. Sci. **45** (1995), 429.
[17] M. Baldo, E.E. Saperstein and S.V. Tolokonnikov, Nucl. Phys. **A 749** (2005), 42.
[18] P. Magierski, A. Bulgac, P.-H. Heenen, Nucl. Phys. **A 719** (2003), 217.
[19] E. Chabanat, P. Bonche, P. Haensel, J. Meyer, R. Schaeffer, Nucl. Phys. **A 635** (1998), 231 ; Erratum, Nucl. Phys. **A 643** (1998), 441.
[20] G.F. Koster, Solid State Physics **5**, edited by F. Seitz, D. Turnbull, Academic Press, New York (1957), 173.
[21] M. Baldo, E.E. Saperstein, S.V. Tolokonnikov, arxiv preprint nucl-th/0609031.
[22] J. Margueron, J. Navarro, and P. Blottiau, Phys. Rev. **C 70**, 028801 (2004).
[23] D. Page, U. Geppert, F. Weber, Nucl. Phys. **A 777** (2006), 497.